# Independent determination of Peltier coefficient in thermoelectric devices

Cite as: Appl. Phys. Lett. **120**, 183901 (2022); doi: 10.1063/5.0093575 Submitted: 29 March 2022 · Accepted: 24 April 2022 · Published Online: 2 May 2022







Ruchika Dhawan, Hari Prasad Panthi, Orlando Lazaro, Andres Blanco, Hal Edwards, nad Mark Lee la la

## **AFFILIATIONS**

- <sup>1</sup>Department of Physics, The University of Texas at Dallas, Richardson, Texas 75080, USA
- <sup>2</sup>Texas Instruments Incorporated, Dallas, Texas 75243, USA

### **ABSTRACT**

Thermoelectric (TE) generators and coolers are one possible solution to energy autonomy for internet-of-things and biomedical electronics and to locally cool high-performance integrated circuits. The development of TE technology requires not only research into TE materials but also advancing TE device physics, which involves determining properties such as the thermopower ( $\alpha$ ) and Peltier ( $\Pi$ ) coefficients at the device rather than material level. Although  $\Pi$  governs TE cooler operation, it is rarely measured because of difficulties isolating  $\Pi$  from larger non-Peltier heat effects such as Joule heating and Fourier thermal conduction. Instead,  $\Pi$  is almost always inferred from  $\alpha$  via a theoretical Kelvin relation  $\Pi = \alpha T$ , where T is the absolute temperature. Here, we demonstrate a method for independently measuring  $\Pi$  on any TE device via the difference in heat flows between the thermopile held open-circuit vs short-circuit. This method determines  $\Pi$  solely from conventionally measured device performance parameters, corrects for non-Peltier heat effects, does not require separate knowledge of material property values, and does not assume the Kelvin relation. A measurement of  $\Pi$  is demonstrated on a commercial Bi $_2$ Te $_3$  TE generator. By measuring  $\alpha$  and  $\Pi$  independently on the same device, the ratio ( $\Pi/\alpha$ ) is free of parasitic thermal impedances, allowing the Kelvin relation to be empirically verified to reasonable accuracy.

Published under an exclusive license by AIP Publishing. https://doi.org/10.1063/5.0093575

Thermoelectric (TE) devices are used as generators (TEGs) to convert heat flow into electrical power output or as coolers (TECs) to provide refrigeration using electrical power input. TE devices are reliable because they have no mechanical parts and are environmentally friendly because TEGs harvest heat that would otherwise be wasted, and TECs use no ecologically damaging refrigerants. Macroscopic TE devices, typically  $\sim 10 \text{ cm}^2$  in cross-sectional area and  $\sim 1 \text{ mm}$  thick, are commercially available. Recently, significant interest has developed in microelectronic TE ( $\mu$ TE) devices, typically < few mm<sup>2</sup> in area and ≤0.1 mm thick, which can be incorporated on-chip or in-package with Si integrated circuits (ICs). μTEGs could provide energy autonomy to power internet-of-things<sup>2-4</sup> and biomedical electronics<sup>5,6</sup> wherever a reliable thermal gradient exists, and  $\mu$ TECs can locally cool hotspots in high-performance ICs<sup>7,8</sup> to reduce the expensive and energy wasteful global air-conditioning needs of modern large data centers.9,10

Most current work advancing TE technology focuses on developing new materials having a high TE figure-of-merit. Equally important to TE technology should be device physics research to optimize TE performance at the device level, especially for  $\mu$ TEs where circuit

parasitics can strongly undermine performance. <sup>12</sup> Understanding TE device physics requires determining basic TE parameters at the device level, principally the electrical and thermal resistances, R and  $\Theta$ , respectively, and the thermopower (Seebeck) and Peltier coefficients,  $\alpha$  and  $\Pi$ . (Here, we take  $\alpha$  to be temperature independent over temperatures of interest and so neglect the Thomson effect, a valid assumption in most common applications.) For devices, one must account for the properties of the TE materials and for parasitic electrical and thermal resistances from contacts and leads.

Although  $\Pi$  governs TEC operation, it is rarely actually measured, <sup>13,14</sup> but is nearly always inferred from measurements of  $\alpha$  using a Kelvin relation <sup>15</sup>  $\Pi = \alpha T$  (depending on author, this may be called the first or second Kelvin relation), where T is the absolute temperature. This is a specific example of an Onsager reciprocal relation (ORR) between generalized forces and flows arising from the assumption of microscopic reversibility in a macroscopic irreversible nonequilibrium thermodynamic process. <sup>16–18</sup> In TE physics, the forces are electric potential and thermal gradients, and the flows are charge and heat currents. <sup>19</sup> In theoretical physics, the ORR and, more specifically, the Kelvin relation are broadly accepted as correct for steady state

a) Author to whom correspondence should be addressed: marklee@utdallas.edu

linear response in systems not too far from equilibrium, although logarithmic corrections have been proposed. <sup>20</sup> Interestingly, in experimental physics, few rigorous tests of the Kelvin relation or ORR exist. <sup>13,14,21</sup>

The lack of independent determination of  $\Pi$  is largely because the Peltier heat flow  $Q_{\text{Pelt}} = \Pi I$ , where I is the electric current through the thermopile, can be difficult to distinguish accurately from Fourier (passive) thermal conduction,  $Q_{\text{Fourier}} = \Delta T/\Theta$ , where  $\Delta T$  is the temperature difference across a TE device, and Joule heating,  $Q_{\text{Joule}} = I^2 R$ , both of which are typically significantly larger than Q<sub>Pelt</sub>. reports on measuring Π using calorimetry on metal-metal thermocouple junctions that are still cited today were done in the late 1800s to early 1900s. 13 These old and some modern 23 Peltier measurements have been criticized14 for neglecting to properly correct for non-Peltier heat transfer effects or for assuming unphysical temperature profiles. More recent efforts to determine  $\Pi$  in semiconductor TE devices involved either measuring the temperature profile along the TE elements of a thermopile<sup>24</sup> or monitoring the time evolution of the temperature difference in a thermopile after applying a current bias.<sup>22</sup> In both these methods, deriving a value for  $\Pi$  also required separate knowledge of constituent material thermal conductivities or emissivities. In addition, both measurements would pose significant technical difficulties to perform on  $\mu TE$  devices, where access to the thermopile would require destructively cross-sectioning the device.

In this paper, we present a method to determine  $\Pi$  in any TE device from conventional performance characteristics that can be measured nondestructively using standard instruments, without relying on the Kelvin relation or separately knowing values of any material property. Here,  $\Pi$  is determined from the difference between the TE circuit's heat flow when the thermopile is held in open-circuit (OC) and short-circuit (SC) conditions as well as measuring the SC current,  $I_{\text{SC}}$ , at fixed applied temperatures. Because no electrical power is input or output from the thermopile under OC or SC conditions, no net Joule heating occurs. Subtraction of SC and OC heat flows isolates  $Q_{\text{Pelt}}$  from  $Q_{\text{Fourier}}$ . This method is demonstrated using a bulk commercial  $\text{Bi}_2\text{Te}_3$  TEG.

A generic semiconductor TE device consisting of a thermopile with n- and p-type TE legs is illustrated in Fig. 1(a). At the top is a heat source assumed to maintain a known temperature  $T_{\text{source}}$ . This source is thermally connected via a thermal contact, with parasitic

thermal resistance  $\Theta_1$ , to the top of the thermopile at temperature  $T_1$ . At the bottom is a heat sink assumed to maintain a known temperature  $T_{\rm sink}$ . This sink is thermally connected, via a thermal contact with parasitic thermal resistance  $\Theta_2$ , to the bottom of the thermopile at temperature  $T_2$ . The thermopile may be electrically connected to an external electrical source or load at voltage  $V_{\rm TP}$  and current  $I_{\rm TP}$ . For a TEG, the power output delivered to a load is  $-V_{\rm TP}I_{\rm TP}$ . For a TEC, the power input needed to refrigerate is  $V_{\rm TP}I_{\rm TP}$ . Using both p- and n-type materials, the device's net intrinsic thermopower is  $\alpha = \alpha_p - \alpha_m$  and the net intrinsic Peltier coefficient is  $\Pi = \Pi_p - \Pi_m$ , where  $\alpha_p$ ,  $\Pi_p > 0$ , and  $\alpha_m$   $\Pi_n < 0$ .

Figures 1(b) and 1(c) depict the heat flow circuit when the thermopile is held (b) OC ( $I_{\rm TP}=0$ ) and (c) SC ( $V_{\rm TP}=0$ ). In both cases,  $V_{\rm TP}I_{\rm TP}=0$ , so no electrical power is delivered to or withdrawn from the thermopile. In steady-state, energy conservation then requires that the same heat flow Q flowing from the heat source through  $\Theta_1$  into the thermopile top must flow through the thermopile and out from the thermopile bottom through  $\Theta_2$  to the heat sink. In OC, there is no electric current, so the OC heat flow  $Q_{\rm OC}$  only flows by Fourier thermal conduction:  $Q_{\rm OC}=\Delta T/\Theta_{\rm tot}$  where  $\Delta T=(T_{\rm source}-T_{\rm sink})$  is the applied temperature difference and  $\Theta_{\rm tot}=(\Theta_1+\Theta_2+\Theta_{\rm TP})$  is the total thermal resistance of the device. Here,  $\Theta_{\rm TP}$  is the thermal resistance of the thermopile, including the TE elements and any parallel (shunt) heat flow through non-TE spacing material such as air or dielectric filler within the thermopile.

The SC heat flow in Fig. 1(c) is more complicated. The temperature difference  $\Delta T_{12} = (T_1 - T_2)$  that appears across the thermopile causes a thermopower potential shift  $^{14}$   $\alpha \Delta T_{12}.$  To maintain  $V_{TP} = 0$ , an SC current  $I_{SC}$  spontaneously flows through the thermopile resistance R, such that  $I_{SC}R = \alpha \Delta T_{12}$ , canceling the thermal potential. At  $T_1$ ,  $I_{SC}$  carries Peltier heat  $\Pi(T_1)I_{SC}$  into the thermopile. At  $T_2$ ,  $I_{SC}$  carries Peltier heat  $\Pi(T_2)I_{SC}$  out of the thermopile. Because no electrical power is input to or output from the thermopile, no net heat is gained or lost within the thermopile, so any difference in these Peltier heat flows is absorbed by the resistor:  $[\Pi(T_1) - \Pi(T_2)]I_{SC} = I_{SC}^2R$ . Solving the Poisson equation for temperature distribution  $^{25,26}$  shows that  $^{1}/_{2}I_{SC}^2R$  flows into  $T_1$  and  $^{1}/_{2}I_{SC}^2R$  flows into  $T_2$ . The  $I_{SC}$ -dependent heat flow from  $T_1$  is then  $\Pi(T_1)I_{SC} - ^{1}/_{2}I_{SC}^2R = ^{1}/_{2}[\Pi(T_1) + \Pi(T_2)]I_{SC}$ , and the  $I_{SC}$ -dependent heat flow out to  $T_2$  is  $\Pi(T_2)I_{SC} + ^{1}/_{2}I_{SC}^2R = ^{1}/_{2}[\Pi(T_1) + \Pi(T_2)]I_{SC}$ . The equality of these heat flows preserves the

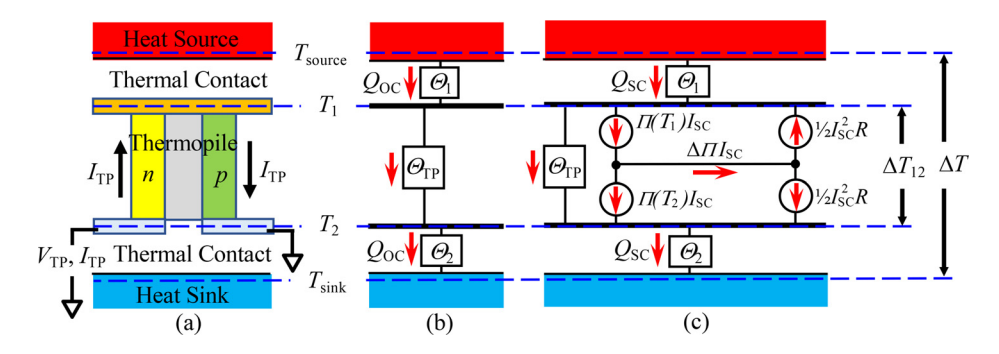


**FIG. 1.** (a) Generic semiconductor TE device with thermopile consisting of n- and p-type legs. Depicted are thermal contacts between thermopile and heat source and heat sink as well as thermopile voltage ( $V_{TP}$ ) and current ( $I_{TP}$ ) connections. (b) and (c) Heat flow circuit when the thermopile is held (b) open-circuit (OC,  $I_{TP}=0$ ) and (c) short circuit (SC,  $V_{TP}=0$ ). Here,  $\Delta\Pi=\Pi(T_1)-\Pi(T_2)$ ,  $\Delta T=T_{\text{source}}-T_{\text{sink}}$  is the applied temperature difference, and  $\Delta T_{12}=T_1-T_2$  is the resulting temperature difference across the thermopile.

requirement that the net SC heat flow  $Q_{\rm SC}$  is the same throughout the device. Using these facts, solving the thermal circuit of Fig. 1(c) gives the SC heat flow,

$$Q_{\rm SC} = \Theta_{\rm tot}^{-1} \Delta T + \left(\frac{\Theta_{\rm TP}}{\Theta_{\rm tot}}\right) \bar{\Pi} I_{\rm SC},\tag{1}$$

where  $\bar{\Pi} = \frac{1}{2}[\Pi(T_1) + \Pi(T_2)]$  is the mean Peltier coefficient of the thermopile operating between  $T_1$  and  $T_2$ . A detailed derivation is given in the supplementary material.

Subtracting the SC and OC heat flows at constant  $T_{\rm sink}$  and  $T_{\rm source}$  gives

$$\bar{\Pi}_{\text{meas}} \equiv \left( \frac{\Theta_{\text{TP}}}{\Theta_{\text{tot}}} \right) \bar{\Pi} = \left. \left( \frac{Q_{\text{SC}} - Q_{\text{OC}}}{I_{\text{SC}}} \right) \right|_{\text{const } T_{\text{sink}}, T_{\text{source}}}, \tag{2}$$

where  $\bar{\Pi}_{\rm meas}$  is the measured value of the Peltier coefficient obtained by measuring  $I_{\rm SC}$  and the difference in heat flows between SC and OC, all using the same  $T_{\rm sink}$  and  $T_{\rm source}$ .  $\bar{\Pi}_{\rm meas}$  corrects for passive thermal conduction, does not involve net Joule heating, does not require knowing values of any material TE properties or the layout of the device under test, and can be determined in a nondestructive manner. However,  $\bar{\Pi}_{\rm meas}$  is reduced from the thermopile's intrinsic  $\bar{\Pi}$  by a factor of  $(\Theta_{\rm TP}/\Theta_{\rm tot})$  that depends on the parasitic series thermal resistances in the TE circuit.

From the simple OC thermal resistor circuit of Fig. 1(b), it is clear that the temperature difference appearing across the thermopile is reduced from the applied temperature difference by  $(\Delta T_{12}/\Delta T) = (\Theta_{TP}/\Theta_{tot})$ . Therefore, the measured thermopower  $\alpha_{meas} \equiv V_{OC}/\Delta T = (\alpha \Delta T_{12})/\Delta T = (\Delta T_{12}/\Delta T)\alpha = (\Theta_{TP}/\Theta_{tot})\alpha$  is reduced from the thermopile's intrinsic  $\alpha$  by the same factor of  $(\Theta_{TP}/\Theta_{tot})$  as  $\bar{\Pi}_{meas}$  is reduced from  $\bar{\Pi}$ . In devices where the parasitic  $(\Theta_1 + \Theta_2)$  is large compared to  $\Theta_{TP}$ , which is often the case for  $\mu$ TE devices,  $\alpha_{meas}$  and  $\bar{\Pi}_{meas}$  can then be significantly smaller than their intrinsic values. However, the ratio  $(\bar{\Pi}_{meas}/\alpha_{meas}) = (\bar{\Pi}/\alpha)$  is independent of

 $(\Theta_{TP}/\Theta_{tot})$ . Consequently,  $\Pi_{meas}$  from (2) combined with a standard  $\alpha_{meas}$  measurement on the same device can be used to test the Kelvin relation free from thermal parasitic resistances, passive thermal conduction, Joule heating, and without needing to know any material properties.

We demonstrate this Peltier measurement on a commercial  $\mathrm{Bi_2Te_3}\text{-}\mathrm{based}$  TEG (Marlow TG12–2.5). From its data sheet  $^{27}$  and values<sup>28</sup> of the TE properties of bulk Bi<sub>2</sub>Te<sub>3</sub>, we estimate that the thermal parasitics of this device are small enough that 0.9 <  $(\Theta_{TP}/\Theta_{tot}) \le 1$ . The test setup is illustrated in Fig. 2(a). The TEG,  $3 \times 3$  cm<sup>2</sup> in area and 4 mm thick, was clamped between an Al heater block having the same area as the TEG and a larger finned Al heat sink that has a fan circulating room air through the fins. The heater block was heated by two resistive heater cartridges embedded in it, connected to the heater output of a temperature controller (Lakeshore 334). The temperature controller supplied voltage  $V_{\rm block}$  and current  $I_{\rm block}$  to the block's heater cartridges, so the Joule heat produced in the block was Qblock  $=V_{\rm block}I_{\rm block}$ . With no thermal leakage to the environment,  $Q_{\rm SC}$  $=Q_{block}$  when the thermopile was short-circuited and  $Q_{OC} = Q_{block}$ when the thermopile was open-circuited. These heat flows were conveniently determined by measuring  $I_{block}$  and  $V_{block}$  using two Keithley 2010 multimeters: one configured as an ammeter [A in Fig. 2(a)] and the other as a voltmeter [V in Fig. 2(a)], connected to the block's heater cartridge leads. To enforce no thermal leakage, the top and sides of the heater block were surrounded by phenolic insulation, which, in turn, was surrounded by an Al heat shield having its own heaters embedded in it. The temperature controller maintained a set temperature on the heater block and kept the shield's temperature within ±0.01 K of the block to minimize thermal leakage from the block to the environment. Using the literature value of the thermal conductivity of the phenolic insulation and the known geometry, we calculated that, of the  $Q_{\rm block}$   $\sim$  0.3 W needed to raise the block temperature by 1 K, no more than 2.3 mW (0.8%) leaks to the environment, so >99% of  $Q_{\rm block}$  flows through the TEG to the heat sink.

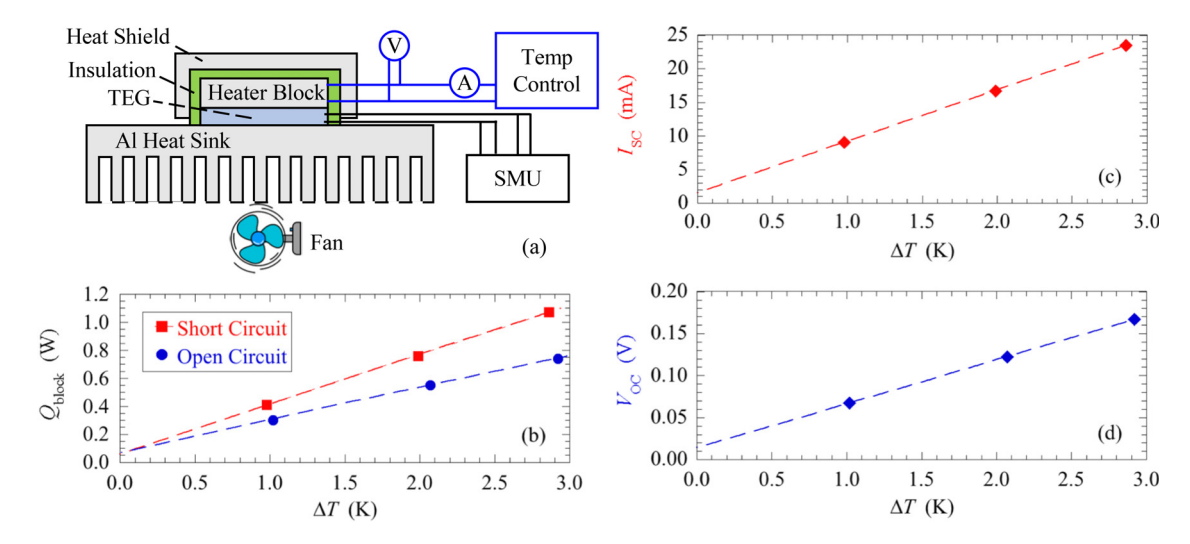


**FIG. 2.** (a) Illustration of the setup to measure mean Peltier coefficient in a TEG. (b) Heat flow from the heater block needed to maintain  $\Delta T \approx 1.0$ , 2.0, and 2.9 K with  $T_{\text{sink}}$  near 296.8 K with the TEG in short circuit (red square) and open circuit (blue circle) conditions. (c) Short circuit current and (d) open circuit voltage across the TEG at same temperature conditions as in (b). In (b), (c), and (d), the dashed lines represent linear fits to the data points.

The temperatures of the heat sink, heater block, and heat shield were monitored by type K thermocouple thermometers inserted within each Al piece so as to be centered on the TEG. A calibration at two physical points by immersion in an ice/water bath and in boiling water was used to adjust each thermometer's offset in order to bring its reading to within  $\pm 0.20\,\mathrm{K}$  of the standard type K temperature curve<sup>29</sup> at 273.15 and 373.15 K. After this adjustment, at both ice bath and ambient room temperatures (approximately 297 K), the heater block and heat shield thermometers agreed with each other to within  $\pm 0.02\,\mathrm{K}$ , and either of those thermometers agreed with the heat sink thermometer to within  $\pm 0.10\,\mathrm{K}$ .

For this demonstration,  $\bar{\Pi}_{\rm meas}$  was determined by measuring  $Q_{\rm SC}$ ,  $Q_{\rm OC}$ , and  $I_{\rm SC}$  using  $\Delta T$  up to 2.90  $\pm$  0.04 K with  $T_{\rm sink}$  constant to within  $\pm$ 0.04 K of 296.8 K. This maximum  $\Delta T$  was kept small because at the heater powers needed to achieve significantly higher  $\Delta T$ ,  $T_{\rm sink}$  could not be maintained nearly constant and began to differ significantly between SC and OC conditions. In these measurements,  $Q_{\rm SC} = Q_{\rm block}$  with thermopile voltage held at  $V_{\rm TP} = 0$  and  $Q_{\rm OC} = Q_{\rm block}$  with thermopile current held at  $I_{\rm TP} = 0$ . SC and OC conditions were forced using a Keithley 2401 source-measure unit (SMU) in four-probe configuration.  $I_{\rm SC}$  was the current sourced by the SMU to maintain  $V_{\rm TP} = 0$ , and  $V_{\rm OC}$  was the voltage sourced by the SMU to maintain  $I_{\rm TP} = 0$ .

With temperatures stable and the TEG held either SC or OC, 40 consecutive measurements of  $V_{\text{block}}$ ,  $I_{\text{block}}$ , and either  $I_{\text{SC}}$  or  $V_{\text{OC}}$  were made, each measurement using integration time of 1.67 s, and subsequently averaged. The largest source of experimental error in determining the values of  $Q_{SC}$ ,  $Q_{OC}$ , and  $I_{SC}$  was systematic error from instrumental offsets, i.e., nonzero residual values of  $V_{block}$ ,  $I_{block}$ , and  $I_{SC}$  when  $\Delta T = 0$ . To determine these offsets as accurately as possible, two additional measurements of  $Q_{SC}$ ,  $Q_{OC}$ , and  $I_{SC}$  were made at intermediate  $\Delta T$  near 1.0 and 2.0 K, and the three data points for each quantity were fit to lines. As shown in Figs. 2(b) and 2(c), the extrapolations back to  $\Delta T = 0$  of the dashed line linear fits to the data give the instrumental offsets for each measurement. From Fig. 2(c), after offset correction, we obtain  $I_{SC} = 0.0220 \pm 0.0003$  A at  $\Delta T = 2.9$  K, with the uncertainty reflecting offset accuracy. Because Q<sub>SC</sub> and Q<sub>OC</sub> were measured using the same instruments, settings, and contact configurations, their systematic errors should be nearly equal and correlated, as evidenced by their nearly identical intercepts in Fig. 2(b). Consequently, the difference  $(Q_{SC} - Q_{OC})$  that goes into (2) is insensitive to systematic errors compared to either  $Q_{SC}$  or  $Q_{OC}$  alone. We obtain  $(Q_{SC} - Q_{OC})$  $= 0.340 \pm 0.002$  W, with the uncertainty reflecting the standard deviation in the 40 measurements of  $V_{\text{block}}I_{\text{block}}$  under SC or OC condition. Using these values in (2) gives  $\bar{\Pi}_{\text{meas}} = (15.5 \pm 0.3) \text{ W A}^{-1}$ 

The measured thermopower  $\alpha_{\rm meas}=0.0522\pm0.0005~{\rm K}^{-1}$  as determined by the slope of the  $V_{\rm OC}$  vs  $\Delta T$  line in Fig. 2(d). This value is about 5% less than the value of  $V_{\rm OC}/\Delta T$  using  $T_{\rm cold}=50~{\rm K}$  and  $T_{\rm hot}=110~{\rm K}$  given in the TEG data sheet. The measured Peltier-to-thermopower ratio is then  $(\bar{\Pi}_{\rm meas}/\alpha_{\rm meas})=(297\pm8)~{\rm K}$ . The Kelvin relation predicts  $(\bar{\Pi}/\alpha)=\bar{T}$ , where  $\bar{T}=^1/_2(T_1+T_2)$  is the mean operating temperature of the thermopile. If the device is symmetric between heat source and sink, so that  $\Theta_1=\Theta_2$ , then  $\bar{T}=^1/_2(T_1+T_2)=^1/_2(T_{\rm source}+T_{\rm sink})=(T_{\rm sink}+^1/_2\Delta T)=298.3~{\rm K}$  using  $T_{\rm sink}=296.8~{\rm K}$  and  $\Delta T=2.9~{\rm K}$ . This theoretical value is within the measurement uncertainty of the experiment, with the most likely value of the measured ratio differing from the theoretical result by about 1 K.

To become widely used as autonomous energy sources or coolers in a broad range of IC applications necessitates further development of  $\mu$ TEs as integrated devices, not just isolated materials. To do so will require the ability to characterize basic TE properties at the device level, preferably in a straightforward manner. The Peltier coefficient  $\Pi$ is an example of a TE property that is rarely measured but is usually inferred from thermopower measurements by assuming a Kelvin relation. We introduce a method to measure  $\Pi$  at the device level that is nondestructive, corrects for non-Peltier heat transfers, and is independent of the Kelvin relation. Because our method uses only standard measurements of TE performance parameters, it is applicable to any TE device and may be particularly suitable for small  $\mu$ TE devices. This method is explicitly demonstrated on a commercial TEG. By measuring Peltier coefficient and thermopower independently on the same TE device, the ratio of Peltierto-thermopower coefficients is independent of parasitic thermal resistances and, thus, could be the basis for precision fundamental tests of the Kelvin relation.

See the supplementary material for a detailed derivation of Eqs. (1) and (2).

Work at the University of Texas at Dallas (UTD) was supported by the U.S. National Science Foundation under Award No. ECCS-1707581 and by Texas Instruments, Inc.

# AUTHOR DECLARATIONS

Conflict of Interest

The authors have no conflicts to disclose.

## **Author Contributions**

R.D. and H.P.P. contributed equally to this work.

#### **DATA AVAILABILITY**

The data that support the findings of this study are available from the corresponding author upon reasonable request.

## **REFERENCES**

```
<sup>1</sup>L. E. Bell, Science 321, 1457 (2008).
```

<sup>&</sup>lt;sup>2</sup>M. Haras and T. Skotnicki, Nano Energy 54, 461 (2018).

<sup>&</sup>lt;sup>3</sup>O. H. Ando, Jr., A. L. O. Maran, and N. C. Henao, Renewable Sustainable Energy Rev. 91, 376 (2018).

<sup>&</sup>lt;sup>4</sup>G. Gadea, M. Pacios, Á. Morata, and A. Tarancón, J. Phys. D **51**, 423001 (2018).

<sup>&</sup>lt;sup>5</sup>A. R. M. Siddique, S. Mahmud, and B. Van Heyst, Renewable Sustainable Energy Rev. 73, 730 (2017).

<sup>&</sup>lt;sup>6</sup>H. R. Lee, N. Furukawa, A. J. Ricco, E. Pop, Y. Cui, and Y. Nishi, Appl. Phys. Lett. 118, 173901 (2021).

<sup>&</sup>lt;sup>7</sup>G. Li, J. G. Fernandez, D. A. Lara Ramos, V. Barati, N. Pérez, I. Soldatov, H. Reith, G. Schierning, and K. Nielsch, Nat. Electron. 1, 555 (2018).

<sup>&</sup>lt;sup>8</sup>J. Yan, X. Liao, D. Yan, and Y. Chen, J. Microelectromech. Syst. 27(1), 1–18 (2018).

<sup>&</sup>lt;sup>9</sup>A. Shehabi, S. J. Smith, N. Horner, I. Azevedo, R. Brown, J. Koomey, E. Masanet, D. Sartor, M. Herrlin, and W. Lintner, "United States Data Center Energy Usage Report," California Publication Report No. LBNL-1005775 (Lawrence Berkeley National Laboratory, Berkeley, 2016).

<sup>&</sup>lt;sup>10</sup>N. Jones, Nature **561**, 163 (2018).

<sup>&</sup>lt;sup>11</sup>J. He and T. M. Tritt, Science 357, eaak9997 (2017).

- <sup>12</sup>R. Dhawan, P. Madusanka, G. Hu, K. Maggio, H. Edwards, and M. Lee, IEEE Trans. Electron Devices 68, 2434 (2021).
- <sup>13</sup>D. G. Miller, Chem. Rev. **60**, 15–37 (1960).
- <sup>14</sup>J. Garrido, J. Phys.: Condens. Matter 21, 155802 (2009).
- 15W. Thomson, Proc. R. Soc. Edinburgh 3, 91–98 (1857).
- <sup>16</sup>L. Onsager, Phys. Rev. **37**, 405 (1931).
- <sup>17</sup>L. Onsager, Phys. Rev. 38, 2265 (1931).
- <sup>18</sup>Y.-C. Hua, T.-W. Xue, and Z.-Y. Guo, Phys. Rev. E **103**, 012107 (2021).
- <sup>19</sup>C. Goupil, W. Seifert, K. Zabrocki, E. Müller, and G. J. Snyder, Entropy 13, 1481 (2011).
- <sup>20</sup>V. A. Drebushchak, J. Therm. Anal. Calorim. **91**, 311 (2008).
- <sup>21</sup>Y. Apertet and C. Goupil, Int. J. Therm. Sci. **104**, 225 (2016).
- <sup>22</sup>J. Garrido and A. Casanovas, J. Electron. Mater. 41, 1990 (2012).

- <sup>23</sup>J. Jiménez, E. Rojas, and M. Zamora, J. Appl. Phys. **56**, 3250 (1984).
- <sup>24</sup>H. Straube, J.-M. Wagner, and O. Breitenstein, Appl. Phys. Lett. 95, 052107 (2009).
- <sup>25</sup>G. S. Nolas, J. Sharp, and H. J. Goldsmid, *Thermoelectrics: Basic Principles and New Materials Developments* (Springer, New York, 2001), Chap. 1.
- <sup>26</sup>Z. Tian, S. Lee, and G. Chen, Annu. Rev. Heat Transfer 17, 425 (2014).
- 27 See Cdn2.hubspot.net/hubfs/547732/Data\_Sheets/TG12-2.5.pdf for "TG12-2.5 Thermoelectric Generator by II-VI Marlow."
- <sup>28</sup>M.-K. Han, Y. Jin, D.-H. Lee, and S.-J. Kim, Materials **10**, 1235 (2017).
- 29 See www.lakeshore.com/docs/default-source/product-downloads/325\_manualf0dc89f86bfb4740aedde9dce6cdf807.pdf?sfvrsn=4eb4bc0a\_1 for "Lakeshore Model 325 Temperature Controller User's Manual (rev. 1.7), Appendix D" (2017).